Supporting Information for:

Computational design of cooperatively acting molecular catalyst systems: carbene based tungsten- or molybdenum-catalysts with rhodium- or iridium-complexes for the ionic hydrogenation of N_2 to NH_3

Totan Mondal[a], Walter Leitner,[a,b] Markus Hölscher[a]*

[a]Institut für Technische und Makromolekulare Chemie, RWTH Aachen University, Worringerweg 2, 52074 Aachen, Germany. E-mail: hoelscher@itmc.rwth-aachen.de, leitner@itmc.rwth-aachen.de

[b]Max Planck Institute for Chemical Energy Conversion, Mülheim an der Ruhr, Germany, E-Mail: walter.leitner@cec.mpg.de

Table of Contents

1. Computational details

The study utilized the Gaussian 16 (Revision B.01)[1] software package with default convergence limits for all quantum chemical computations. Standard algorithms implemented in the Gaussian16 program were used to locate necessary geometries (minima and transition states), i.e., the GEDIIS algorithm for minimization and the Berny algorithm code for the transition state. Geometry optimizations were performed without symmetry constraints in an implicit solvent environment to accurately replicate experimental conditions. To account for the influence of acetonitrile solvent ($\varepsilon = 36.64$), the self-consistent reaction field (SCRF) technique based on the SMD[2] continuum solvation model was used. The B97 density functional combined with the Becke-Johnson damping enhanced Grimme D3-dispersion correction (B97-D3(BJ))[3–6] was used to assess the influence of dispersion on geometry and energy. The Ahlrich's formulated triple-ζ basis set (def2-TZVP)[7–9], coupled with the related ECP[10] for the metal centers, was used to build wavefunctions for the systems under investigation.

Furthermore, vibration frequency calculations were performed on the converged geometries using the same theoretical level to verify whether actual minima ($N_{img} = 0$) or saddle points ($N_{img} = 1$) were reached and to obtain necessary thermodynamic energy corrections. Moreover, a pressure correction of 471 atm was applied to align with standard state conditions for acetonitrile. Numerical integrations during computations used an ultrafine grid (99,950). To verify accurate imaginary modes, a visual inspection of the vibrational direction of the pertinent atoms was conducted. In cases of ambiguity, additional IRC (Intrinsic Reaction Coordinate) calculations were conducted to authenticate true transition states.

Discussions throughout the manuscript focused on B97-D3BJ/def2-TZVP/IEFPCM and SMD (acetonitrile) free energies (ΔG), unless specified otherwise. All optimized structures are available as mol files in a separate document for reference.

2. DFT functional test

The selection of the B97D3-BJ functional for this study was primarily based on its computational efficiency and its consistency with our prior investigations into metal-ligand complexes, aligning well with experimental findings. However, we undertook a comprehensive comparative study that included other DFT functionals, specifically PBE0-D3BJ[11,12], B3LYP-D3BJ[11,13,14], and M06-L[15]. To accomplish this, we fully optimized the critical intermediates and transition states of the catalyst **W-L1^{Rh}** in an acetonitrile solvent environment, investigating the changes in energy span.

Notably, all the functionals yielded similar trends, with **TS10** consistently exhibiting higher energy than **TS8**, and intermediate **16** displaying significant stabilities (Figure S1). The energy span calculated using PBE0-D3BJ was approximately 3 kcal/mol lower compared to the values computed with B97D3-BJ. In contrast, the other two functionals showed relatively higher energy spans of 3.6 kcal/mol, which remained within the acceptable range of DFT error. Consequently, we proceeded with the B97D3-BJ computed values for further comparison and a more in-depth understanding of the entire catalytic cycle.
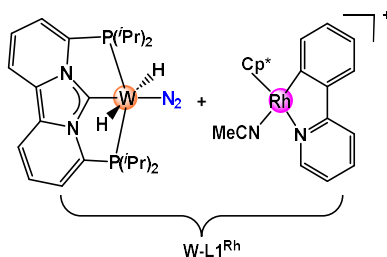
W-L1^{Rh}	B97D3-BJ	PBE0-D3BJ	B3LYP-D3BJ	M06L
1'	0.0	0.0	0.0	0.0
TS8	29.1	13.8	21.7	29.5
TS10	31.6	23.2	27.5	37.0
16	-21.0	-41.9	-35.8	-27.0
ES	32.4	29.3	37.0	37.0

Fig. S1 Relative Gibbs free energies ΔG (kcal/mol) of the selected intermediates and transition states for the **W-L1^{Rh}** catalyst system, computed at various DFT levels.

3 End-on (Ln-1^E) vs. side-on (Ln-1^S) coordination

The relative stability differences between end-on and side-on N$_2$ tungsten complexes was checked for completeness. Depending on the ligand chosen the energy differences can be as low as 3.5 kcal/mol (**L12**) in favor of the end-on complex. Therefore, it is not impossible to envision that by choosing an appropriate ligand (even if it was chosen accidentally) the side-on bonded complex might be more stable. This in turn could have consequences with regard to the catalytic cycle. However, as our results show, this possibility does not come into play with the ligands chosen in this work.
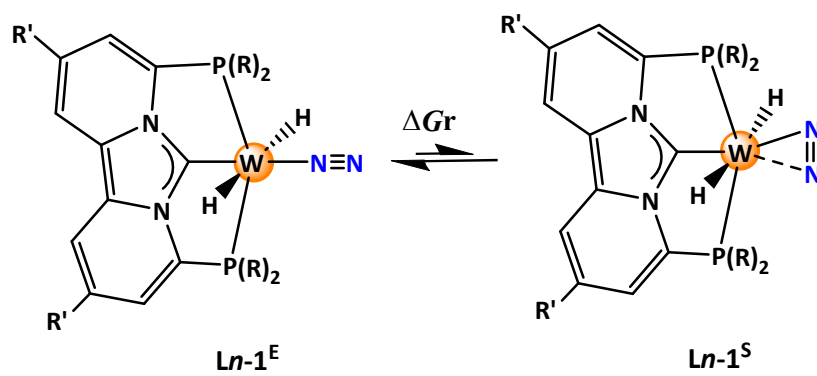
Ln	R	R'	ΔG_r
L1	^{i}Pr	H	17.8
L2	^{t}Bu	H	8.5
L3	Ph	H	15.7
L4	Ph(p-CF$_3$)	H	3.6
L5	Ph(p-F)	H	4.8
L6	Ph(p-Me)	H	6.1
L7	Mes	H	11.0
L8	Ph(p-NMe$_2$)	H	6.1
L9	CF$_3$	H	13.7
L10	^{i}Pr	Me	18.3
L11	^{i}Pr	F	17.7
L12	Ph(p-CF$_3$)	Me	3.5

Fig. S2 Relative Gibbs free energies ΔG_r (kcal/mol) of various end-on (**Ln-1^E**) N$_2$ coordinated tungsten pincer complexes compare to side-on (**Ln-1^S**) N$_2$ coordinated complexes.

4 Full catalytic cycle for the catalytic systems W-L4^{Rh} and W-L7^{Rh}
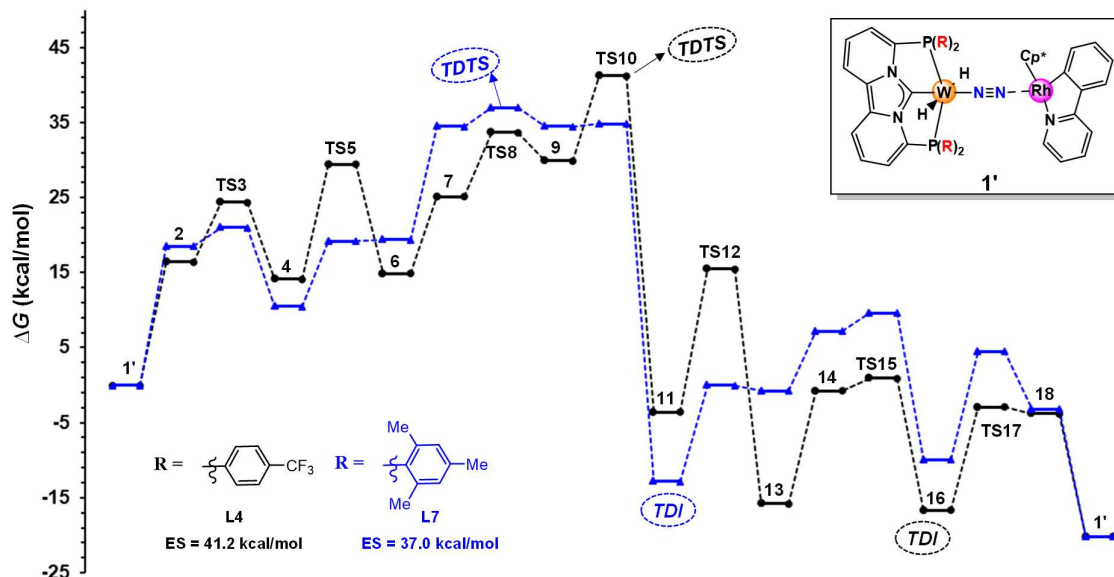
Fig. S3 Minimum energy pathway for the direct hydrogenation of N_2 to NH_3 for the catalysts **W-L4^{Rh}** and **W-L7^{Rh}**, calculated at the B97D3-BJ/def2-TZVP/IEF-PCM, SMD(CH_3CN) level of theory. The relative Gibbs free energies (ΔG) are in kcal/mol.

5 Reaction energetics associated with molybdenum pincer complexes
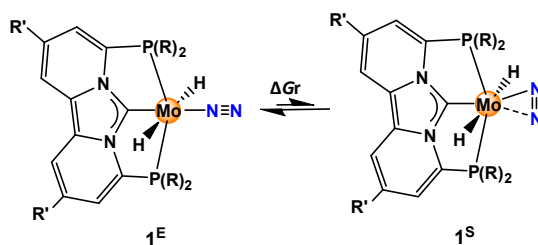
Ln	R	R'	ΔGr (kcal/mol)
L1	^{i}Pr	H	18.4
L2	^{t}Bu	H	9.9
L10	^{i}Pr	Me	18.4
L11	^{i}Pr	F	16.5

Fig. S4 Relative Gibbs free energies ΔGr (kcal/mol) of various end-on (**Ln-1^E**) N_2 coordinated molybdenum pincer complexes compare to side-on (**Ln-1^S**) N_2 coordinated complexes.
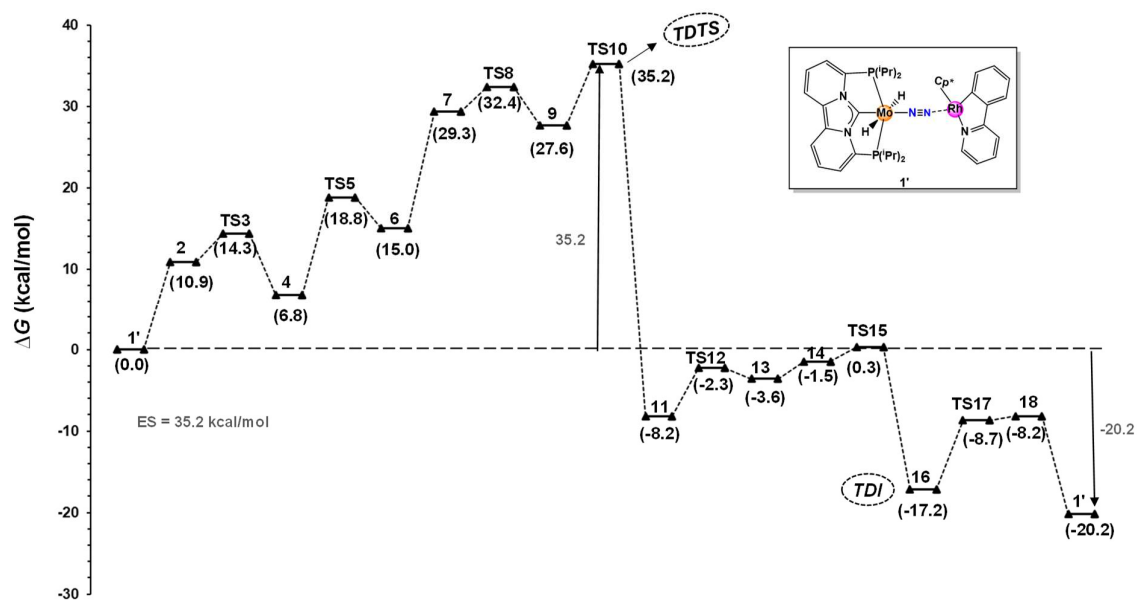
Fig. S5 Minimum energy pathway for the catalyst **Mo-L1^{Rh}**, calculated at the B97D3-BJ/def2-TZVP/IEF-PCM, SMD(CH$_3$CN) level of theory.

6   Different spin states
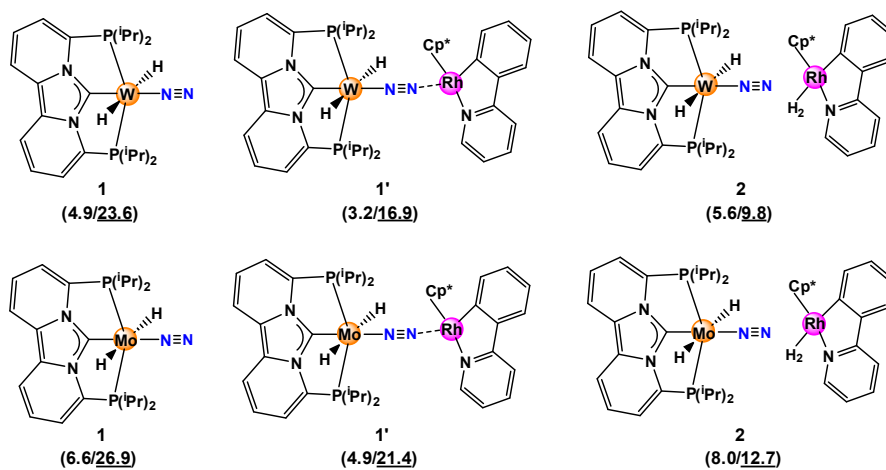
Fig. S6 Relative Gibbs free energies ΔG (kcal/mol) of the **triplet/<u>quintet</u>** spin states with respect to the singlet spin state, computed at the B97D3-BJ/def2-TZVP/IEF-PCM, SMD(CH$_3$CN) level of theory.

7 Solvent effects

Table S1 Relative Gibbs free energies (in kcal/mol) of selected stationary points of the catalytic cycle shown in Scheme 2 with tungsten/molybdenum complexes containing the ligand **L1** in two different solvents.

	W-L1[Rh]			
	TS8	TS10	16	ES[a]
Acetonitrile	29.1	31.6	-21.0	32.4
Dimethylsulfoxide	30.1	33.3	-19.8	33.3
	Mo-L1[Rh]			
Acetonitrile	32.4	35.2	-17.2	35.2
Dimethylsulfoxide	33.9	35.6	-16.8	35.6

[a] ES = energy span; ΔGr = -20.2 kcal/mol [reaction Gibbs free in acetonitrile solvent]; ΔGr = -20.4 kcal/mol [reaction Gibbs free in dimethylsulfoxide solvent]

8 Possible side reactions

M^1 = W
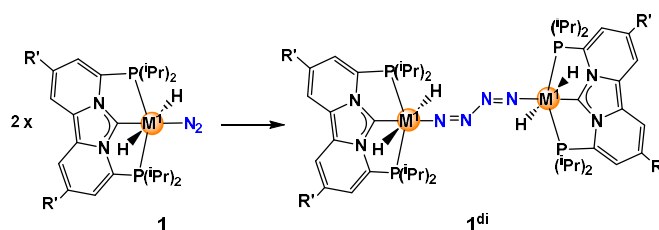
Ln	R'	ΔG
L1	H	45.0
L10	Me	44.5
L11	F	45.8

M^1 = Mo

L1	H	55.3
L10	Me	55.4
L11	F	56.7

Fig. S7 Relative Gibbs free energies ΔG (kcal/mol) for the dimerization reaction **1→1^{di}**.

M¹ = W
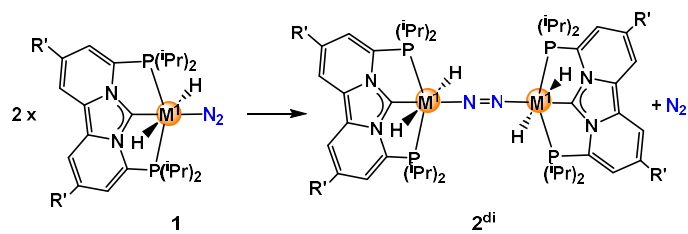
L*n*	R′	Δ*G*
L1	H	-13.7
L10	Me	-13.8
L11	F	-12.9

M¹ = Mo

L1	H	-6.1
L10	Me	-5.2
L11	F	-4.7

Fig. S8 Relative Gibbs free energies Δ*G* (kcal/mol) for the dimerization reaction **1→2^{di}**.
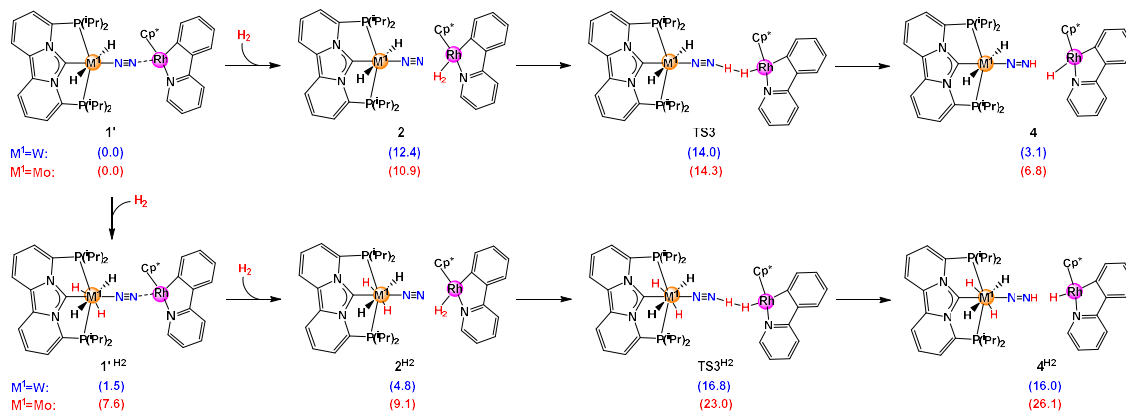
Fig. S9 Relative Gibbs free energies Δ*G* (kcal/mol) calculated at the B97D3-BJ/def2-TZVP/IEF-PCM, SMD(CH₃CN) level of theory.

9 Calculated energies in detail

Table S2 Computed energies (E), zero-point energy corrected energies (E_{zpe}), enthalpies (H) and Gibbs free energies (G; all in Hartree, at the B97D3-BJ/def2-TZVP/IEF-PCM, SMD(CH_3CN) level of theory) of various end-on (**L*n*-1^E**) and side-on (**L*n*-1^S**) N_2 coordinated tungsten pincer complexes as shown in Fig.S1 of the main paper. Relative Gibbs free reaction energies are given as well (ΔG_{rel}; in kcal/mol).

Compd.	E	E_{zpe}	H	G	ΔG_{rel}
L1-1^E	-1866.972491	-1866.435345	-1866.399919	-1866.493205	
L1-1^S	-1866.943744	-1866.407839	-1866.372131	-1866.464918	17.8
L2-1^E	-2024.168439	-2023.521282	-2023.480778	-2023.581493	
L2-1^S	-2024.156045	-2023.508489	-2023.468359	-2023.56788	8.5
L3-1^E	-2319.246871	-2318.723968	-2318.686867	-2318.788816	
L3-1^S	-2319.219842	-2318.697156	-2318.65908	-2318.763723	15.7
L4-1^E	-3667.3497	-3666.811477	-3666.758568	-3666.902695	
L4-1^S	-3667.343214	-3666.805575	-3666.752608	-3666.89696	3.6
L5-1^E	-2716.185914	-2715.695758	-2715.654457	-2715.766564	
L5-1^S	-2716.17798	-2715.687838	-2715.646567	-2715.758917	4.8
L6-1^E	-2476.477609	-2475.84821	-2475.802626	-2475.926883	
L6-1^S	-2476.46918	-2475.83957	-2475.794151	-2475.917122	6.1
L7-1^E	-2790.90671	-2790.058587	-2790.001186	-2790.143642	
L7-1^S	-2790.88827	-2790.040564	-2789.983265	-2790.126079	11.0
L8-1^E	-2855.01463	-2854.206619	-2854.150363	-2854.297859	
L8-1^S	-2855.004762	-2854.197468	-2854.141294	-2854.288087	6.1
L9-1^E	-2743.348701	-2743.127745	-2743.093682	-2743.189406	
L9-1^S	-2743.329408	-2743.107319	-2743.0736	-2743.167534	13.7
L10-1^E	-1945.5877	-1944.996988	-1944.957885	-1945.059379	
L10-1^S	-1945.558679	-1944.968938	-1944.929594	-1945.03016	18.3
L11-1^E	-2065.43536	-2064.914959	-2064.87759	-2064.975221	
L11-1^S	-2065.406744	-2064.88748	-2064.849779	-2064.947045	17.7
L12-1^E	-3745.964844	-3745.372845	-3745.316433	-3745.468236	
L12-1^S	-3745.95852	-3745.36764	-3745.310775	-3745.462666	3.5

Table S3 Computed energies (E), zero-point energy corrected energies (E_{zpe}), enthalpies (H) and Gibbs free energies (G; all in Hartree) for the acetonitrile replacement reaction from the rhodium complex for the various tungsten pincer-ligand complexes as shown in Fig. 1 of the main paper. Relative Gibbs free reaction energies are given as well (ΔG_{rel}; in kcal/mol).

Compd.	E	E_{zpe}	H	G	ΔG_{rel}
Rh-cp	-1112.12527	-1111.704187	-1111.675381	-1111.755821	
MeCN	-132.7304319	-132.686275	-132.681719	-132.704476	
L1-1^E	-1866.972491	-1866.435345	-1866.399919	-1866.493205	
W-L1^{Rh}-1'	-2846.386837	-2845.471761	-2845.41274	-2845.555253	-6.7
L2-1^E	-2024.168439	-2023.521282	-2023.480778	-2023.581493	
W-L2^{Rh}-1'	-3003.586048	-3002.560026	-3002.495228	-3002.647537	-9.2
L3-1^E	-2319.246871	-2318.723968	-2318.686867	-2318.788816	
W-L3^{Rh}-1'	-3298.679193	-3297.778365	-3297.716175	-3297.870248	-18.9
L4-1^E	-3667.3497	-3666.811477	-3666.758568	-3666.902695	
W-L4^{Rh}-1'	-4646.781917	-4645.864704	-4645.787789	-4645.981044	-16.9
L5-1^E	-2716.185914	-2715.695758	-2715.654457	-2715.766564	
W-L5^{Rh}-1'	-3695.619126	-3694.750386	-3694.684947	-3694.846541	-18.0
L6-1^E	-2476.477609	-2475.84821	-2475.802626	-2475.926883	
W-L6^{Rh}-1'	-3455.910815	-3454.902788	-3454.833951	-3455.00451	-16.5
L7-1^E	-2790.90671	-2790.058587	-2790.001186	-2790.143642	
W-L7^{Rh}-1'	-3770.333214	-3769.107969	-3769.02612	-3769.220511	-16.0
L8-1^E	-2855.01463	-2854.206619	-2854.150363	-2854.297859	
W-L8^{Rh}-1'	-3834.451297	-3833.265588	-3833.18509	-3833.381038	-20.0
L9-1^E	-2743.348701	-2743.127745	-2743.093682	-2743.189406	
W-L9^{Rh}-1'	-3722.75853	-3722.160343	-3722.10177	-3722.249529	-5.5
L1-10^E	-1945.5877	-1944.996988	-1944.957885	-1945.059379	
W-L10^{Rh}-1'	-2925.003056	-2924.034458	-2923.970853	-2924.124567	-8.7
L1-11^E	-2065.43536	-2064.914959	-2064.87759	-2064.975221	
W-L11^{Rh}-1'	-3044.848991	-3043.95056	-3043.888706	-3044.038853	-7.7
L1-12^E	-3745.964844	-3745.372845	-3745.316433	-3745.468236	
W-L12^{Rh}-1'	-4725.398345	-4724.42757	-4724.34692	-4724.546747	-17.0

Table S4 Computed energies (E), zero-point energy corrected energies (E_{zpe}), enthalpies (H) and Gibbs free energies (G; all in Hartree) of the different stationary points as shown in Fig. 2 of the main paper.

Compd.	E	E_{zpe}	H	G	ΔG_{rel}
H$_2$	-1.1829428	-1.173025	-1.16972	-1.17871	
W-L1^{Rh}-1'	-2846.386837	-2845.471761	-2845.41274	-2845.555253	
W-L1^{Rh}-TS8	-2848.728621	-2847.778916	-2847.717604	-2847.866303	29.1
W-L2^{Rh}-1'	-3003.586048	-3002.560026	-3002.495228	-3002.647537	
W-L2^{Rh}-TS8	-3005.923822	-3004.864479	-3004.79788	-3004.956887	30.2
W-L3^{Rh}-1'	-3298.679193	-3297.778365	-3297.716175	-3297.870248	
W-L3^{Rh}-TS8	-3301.015338	-3300.077921	-3300.01477	-3300.173687	33.9
W-L4^{Rh}-1'	-4646.781917	-4645.864704	-4645.787789	-4645.981044	
W-L4^{Rh}-TS8	-4649.121122	-4648.167621	-4648.089693	-4648.284719	33.7
W-L5^{Rh}-1'	-3695.619126	-3694.750386	-3694.684947	-3694.846541	
W-L5^{Rh}-TS8	-3697.954642	-3697.050777	-3696.983996	-3697.15123	33.1
W-L6^{Rh}-1'	-3455.910815	-3454.902788	-3454.833951	-3455.00451	
W-L6^{Rh}-TS8	-3458.247606	-3457.203876	-3457.1332	-3457.308307	33.6
W-L7^{Rh}-1'	-3770.333214	-3769.107969	-3769.02612	-3769.220511	
W-L7^{Rh}-TS8	-3772.665223	-3771.405054	-3771.321868	-3771.519012	37.0
W-L8^{Rh}-1'	-3834.451297	-3833.265588	-3833.18509	-3833.381038	
W-L8^{Rh}-TS8	-3836.787641	-3835.566236	-3835.484618	-3835.684	34.2
W-L9^{Rh}-1'	-3722.75853	-3722.160343	-3722.10177	-3722.249529	
W-L9^{Rh}-TS8	-3725.106069	-3724.471319	-3724.41193	-3724.561511	28.5
W-L10^{Rh}-1'	-2925.003056	-2924.034458	-2923.970853	-2924.124567	
W-L10^{Rh}-TS8	-2927.344065	-2926.340713	-2926.275728	-2926.432867	30.8
W-L11^{Rh}-1'	-3044.848991	-3043.95056	-3043.888706	-3044.038853	
W-L11^{Rh}-TS8	-3047.190435	-3046.257139	-3046.193998	-3046.346847	31.0
W-L12^{Rh}-1'	-4725.398345	-4724.42757	-4724.34692	-4724.546747	
W-L12^{Rh}-TS8	-4727.736779	-4726.729703	-4726.64811	-4726.849959	34.0

Table S5 Computed energies (E), zero-point energy corrected energies (E_{zpe}), enthalpies (H) and Gibbs free energies (G; all in Hartree) of the different stationary points involved in the direct hydrogenation of N_2 to NH_3 utilizing the catalyst **W-L1^{Rh}**, as shown in Fig. 3 of the main paper.

Compd.	E	E_{zpe}	H	G	ΔG_{rel}
H$_2$	-1.1829428	-1.173025	-1.16972	-1.17871	
N$_2$	-109.4988745	-109.493463	-109.490158	-109.506089	
NH$_3$	-56.5583513	-56.524939	-56.521127	-56.537173	
W-L1^{Rh}-1'	-2846.386837	-2845.471761	-2845.41274	-2845.555253	
W-L1^{Rh}-2	-2847.558247	-2846.627689	-2846.566725	-2846.71422	12.4
W-L1^{Rh}-TS3	-2847.552404	-2846.62469	-2846.564181	-2846.711683	14.0
W-L1^{Rh}-4	-2847.574311	-2846.641092	-2846.579944	-2846.729038	3.1
W-L1^{Rh}-TS5	-2847.552884	-2846.623992	-2846.562718	-2846.712814	13.3
W-L1^{Rh}-6	-2847.568203	-2846.631483	-2846.570504	-2846.719861	8.8
W-L1^{Rh}-7	-2848.73645	-2847.784624	-2847.722733	-2847.872055	25.5
W-L1^{Rh}-TS8	-2848.728621	-2847.778916	-2847.717604	-2847.866303	29.1
W-L1^{Rh}-9	-2848.74033	-2847.786112	-2847.724497	-2847.875864	23.1
W-L1^{Rh}-TS10	-2848.7251	-2847.772405	-2847.710254	-2847.86233	31.6
W-L1^{Rh}-11	-2792.23145	-2791.313849	-2791.253625	-2791.403084	-17.3
W-L1^{Rh}-TS12	-2792.220237	-2791.305859	-2791.246737	-2791.389753	-8.9
W-L1^{Rh}-13	-2792.226008	-2791.308595	-2791.248517	-2791.395866	-12.8
W-L1^{Rh}-14	-2793.4123	-2792.478652	-2792.417496	-2792.566721	-7.9
W-L1^{Rh}-TS15	-2793.408789	-2792.478246	-2792.417183	-2792.565693	-7.2
W-L1^{Rh}-16	-2793.442194	-2792.502906	-2792.442712	-2792.587681	-21.0
W-L1^{Rh}-TS17	-2793.421995	-2792.484472	-2792.424497	-2792.569571	-9.6
W-L1^{Rh}-18	-2793.427345	-2792.484395	-2792.424421	-2792.56986	-9.8

Table S6 Computed energies (E), zero-point energy corrected energies (E_{zpe}), enthalpies (H) and Gibbs free energies (G; all in Hartree) of the selected stationary points as shown in Table 1 of the main paper.

Ligand	Compd.	E	E_{zpe}	H	G	ΔG_{rel}
	H_2	-1.1829428	-1.173025	-1.16972	-1.17871	
L2	W-L2^{Rh}-1'	-3003.586048	-3002.560026	-3002.495228	-3002.647537	
	W-L2^{Rh}-TS8	-3005.923822	-3004.864479	-3004.79788	-3004.956887	30.2
	W-L2^{Rh}-TS10	-3005.92531	-3004.861961	-3004.795216	-3004.952692	32.8
	W-L2^{Rh}-16	-2950.638071	-2949.58913	-2949.523653	-2949.677856	-19.7
L3	W-L3^{Rh}-1'	-3298.679193	-3297.778365	-3297.716175	-3297.870248	
	W-L3^{Rh}-TS8	-3301.015338	-3300.077921	-3300.01477	-3300.173687	33.9
	W-L3^{Rh}-TS10	-3301.006307	-3300.066772	-3300.002765	-3300.161643	41.4
	W-L3^{Rh}-16	-3245.733261	-3244.805347	-3244.74327	-3244.894875	-16.1
L4	W-L4^{Rh}-1'	-4646.781917	-4645.864704	-4645.787789	-4645.981044	
	W-L4^{Rh}-TS8	-4649.121122	-4648.167621	-4648.089693	-4648.284719	33.7
	W-L4^{Rh}-TS10	-4649.110386	-4648.154906	-4648.076041	-4648.272839	41.2
	W-L4^{Rh}-16	-4593.836675	-4592.893383	-4592.81627	-4593.006631	-16.7
L5	W-L5^{Rh}-1'	-3695.619126	-3694.750386	-3694.684947	-3694.846541	
	W-L5^{Rh}-TS8	-3697.954642	-3697.050777	-3696.983996	-3697.15123	33.1
	W-L5^{Rh}-TS10	-3697.945427	-3697.038436	-3696.971284	-3697.137195	41.9
	W-L5^{Rh}-16	-3642.671041	-3641.77812	-3641.712446	-3641.872648	-17.0
L6	W-L6^{Rh}-1'	-3455.910815	-3454.902788	-3454.833951	-3455.00451	
	W-L6^{Rh}-TS8	-3458.247606	-3457.203876	-3457.1332	-3457.308307	33.6
	W-L6^{Rh}-TS10	-3458.238635	-3457.192709	-3457.121244	-3457.298193	40.0
	W-L6^{Rh}-16	-3402.964666	-3401.930866	-3401.860777	-3402.033273	-18.7
L7	W-L7^{Rh}-1'	-3770.333214	-3769.107969	-3769.02612	-3769.220511	
	W-L7^{Rh}-TS8	-3772.665223	-3771.405054	-3771.321868	-3771.519012	37.0
	W-L7^{Rh}-TS10	-3772.675798	-3771.410615	-3771.328036	-3771.522458	34.8
	W-L7^{Rh}-16	-3717.373635	-3716.122897	-3716.040492	-3716.235259	-9.9
L8	W-L8^{Rh}-1'	-3834.451297	-3833.265588	-3833.18509	-3833.381038	
	W-L8^{Rh}-TS8	-3836.787641	-3835.566236	-3835.484618	-3835.684	34.2
	W-L8^{Rh}-TS10	-3836.780594	-3835.55704	-3835.474761	-3835.674371	40.2
	W-L8^{Rh}-16	-3781.504828	-3780.293341	-3780.212276	-3780.408317	-17.8
L9	W-L9^{Rh}-1'	-3722.75853	-3722.160343	-3722.10177	-3722.249529	
	W-L9^{Rh}-TS8	-3725.106069	-3724.471319	-3724.41193	-3724.561511	28.5
	W-L9^{Rh}-TS10	-3725.086132	-3724.448493	-3724.388115	-3724.540765	41.5
	W-L9^{Rh}-16	-3669.816445	-3669.189765	-3669.131655	-3669.275603	-17.0
L10	W-L10^{Rh}-1'	-2925.003056	-2924.034458	-2923.970853	-2924.124567	

	W-L10^{Rh}-TS8	-2927.344065	-2926.340713	-2926.275728	-2926.432867	30.8
	W-L10^{Rh}-TS10	-2927.34149	-2926.336111	-2926.270143	-2926.430426	32.4
	W-L10^{Rh}-16	-2872.057544	-2871.065625	-2871.001323	-2871.156619	-20.8
L11	W-L11^{Rh}-1'	-3044.848991	-3043.95056	-3043.888706	-3044.038853	
	W-L11^{Rh}-TS8	-3047.190435	-3046.257139	-3046.193998	-3046.346847	31.0
	W-L11^{Rh}-TS10	-3047.186725	-3046.251623	-3046.187402	-3046.344095	32.7
	W-L11^{Rh}-16	-2991.90331	-2990.981031	-2990.91874	-2991.06924	-19.7
L12	W-L12^{Rh}-1'	-4725.398345	-4724.42757	-4724.34692	-4724.546747	
	W-L12^{Rh}-TS8	-4727.736779	-4726.729703	-4726.64811	-4726.849959	34.0
	W-L12^{Rh}-TS10	-4727.72717	-4726.717856	-4726.63542	-4726.840885	39.7
	W-L12^{Rh}-16	-4672.452925	-4671.456981	-4671.376453	-4671.574341	-18.0

Table S7 Computed energies (E), zero-point energy corrected energies (E$_{zpe}$), enthalpies (H) and Gibbs free energies (G; all in Hartree) of the selected stationary points as shown in Table 2 of the main paper.

Ligand	Compd.	E	E$_{zpe}$	H	G	ΔG_{rel}
	H$_2$	-1.1829428	-1.173025	-1.16972	-1.17871	
L1	Mo-L1^{Rh}-1'	-2847.490266	-2846.574788	-2846.515182	-2846.659484	
	Mo-L1^{Rh}-TS8	-2849.826019	-2848.876877	-2848.815435	-2848.965217	32.4
	Mo-L1^{Rh}-TS10	-2849.824887	-2848.872202	-2848.810237	-2848.960775	35.2
	Mo-L1^{Rh}-16	-2794.539502	-2793.600664	-2793.540385	-2793.68578	-17.2
L2	Mo-L2^{Rh}-1'	-3004.689404	-3003.663868	-3003.598957	-3003.751898	
	Mo-L2^{Rh}-TS8	-3007.023251	-3005.963093	-3005.896829	-3006.054635	34.3
	Mo-L2^{Rh}-TS10	-3007.024487	-3005.960861	-3005.894277	-3006.051392	36.3
	Mo-L2^{Rh}-16	-2951.736564	-2950.687614	-2950.622305	-2950.775838	-15.7
L10	Mo-L10^{Rh}-1'	-2926.10634	-2925.13728	-2925.074035	-2925.225866	
	Mo-L10^{Rh}-TS8	-2928.441718	-2927.439731	-2927.374379	-2927.533714	31.1
	Mo-L10^{Rh}-TS10	-2928.441323	-2927.436097	-2927.370125	-2927.530334	33.2
	Mo-L10^{Rh}-16	-2873.155292	-2872.163227	-2872.099115	-2872.254047	-18.3
L11	Mo-L11^{Rh}-1'	-3045.95249	-3045.053768	-3044.992284	-3045.140229	
	Mo-L11^{Rh}-TS8	-3048.287909	-3047.355849	-3047.29233	-3047.447648	31.4
	Mo-L11^{Rh}-TS10	-3048.286547	-3047.351298	-3047.287147	-3047.44338	34.1
	Mo-L11^{Rh}-16	-2993.000935	-2992.079045	-2992.01669	-2992.168038	-18.1

Table S8 Computed energies (E), zero-point energy corrected energies (E_{zpe}), enthalpies (H) and Gibbs free energies (G; all in Hartree) of the selected stationary points as shown in Table 3 of the main paper.

Ligand	Compd.	E	E_{zpe}	H	G	ΔG_{rel}
	H₂	-1.1829428	-1.173025	-1.16972	-1.17871	
L1	W-L1^{Ir}-1'	-2840.188127	-2839.272121	-2839.21256	-2839.357094	
	W-L1^{Ir}-TS8	-2842.53909	-2841.591104	-2841.529025	-2841.679882	21.7
	W-L1^{Ir}-TS10	-2842.53484	-2841.582015	-2841.519774	-2841.671863	26.8
	W-L1^{Ir}-16	-2787.251406	-2786.311912	-2786.251607	-2786.397622	-26.1
L10	W-L10^{Ir}-1'	-2918.804114	-2917.834735	-2917.771504	-2917.923604	
	W-L10^{Ir}-TS8	-2921.156742	-2920.153053	-2920.088314	-2920.244932	22.6
	W-L10^{Ir}-TS10	-2921.151209	-2920.145904	-2920.079736	-2920.240864	25.2
	W-L10^{Ir}-16	-2865.867277	-2864.874248	-2864.810324	-2864.963863	-25.9
L11	W-L11^{Ir}-1'	-3038.650173	-3037.751082	-3037.689573	-3037.838454	
	W-L11^{Ir}-TS8	-3041.003255	-3040.069777	-3040.006774	-3040.159116	23.1
	W-L11^{Ir}-TS10	-3040.996456	-3040.061443	-3039.996999	-3040.155898	25.1
	W-L11^{Ir}-16	-2985.713099	-2984.790585	-2984.728348	-2984.878363	-25.7
L1	Mo-L1^{Ir}-1'	-2841.291495	-2840.376014	-2840.316596	-2840.459717	
	Mo-L1^{Ir}-TS8	-2843.639071	-2842.68883	-2842.627801	-2842.775666	26.0
	Mo-L1^{Ir}-TS10	-2843.634622	-2842.682093	-2842.619863	-2842.771654	28.5
	Mo-L1^{Ir}-16	-2788.348874	-2787.409772	-2787.349439	-2787.494808	-22.7
L10	Mo-L10^{Ir}-1'	-2919.907406	-2918.938222	-2918.875153	-2919.026161	
	Mo-L10^{Ir}-TS8	-2922.254475	-2921.250958	-2921.186142	-2921.342674	25.7
	Mo-L10^{Ir}-TS10	-2922.25106	-2921.245577	-2921.179557	-2921.339973	27.4
	Mo-L10^{Ir}-16	-2866.964776	-2865.972725	-2865.909408	-2866.060939	-22.5
L11	Mo-L11^{Ir}-1'	-3039.753677	-3038.854822	-3038.79355	-3038.940584	
	Mo-L11^{Ir}-TS8	-3042.100921	-3041.16762	-3041.104564	-3041.25725	25.6
	Mo-L11^{Ir}-TS10	-3042.096277	-3041.16104	-3041.096752	-3041.253531	27.9
	Mo-L11^{Ir}-16	-2986.810704	-2985.887651	-2985.825627	-2985.976065	-22.9

Table S9 Computed energies (E), zero-point energy corrected energies (E_{zpe}), enthalpies (H) and Gibbs free energies (G; all in Hartree) of the selected stationary points as shown in Table 4 of the main paper.

Compd.	E	E_{zpe}	H	G	ΔG_{rel}
H_2	-1.1829428	-1.173025	-1.16972	-1.17871	
W-L1^{Rh}-Cl-1'	-3765.78326	-3764.880239	-3764.816983	-3764.969074	
W-L1^{Rh}-Cl-TS8	-3768.140359	-3767.200083	-3767.136176	-3767.290512	22.6
W-L1^{Rh}-Cl-TS10	-3768.130229	-3767.187721	-3767.123034	-3767.278201	30.3
W-L1^{Rh}-Cl-16	-3712.842879	-3711.915733	-3711.852015	-3712.006503	-24.1
W-L1^{Rh}-N-1'	-3064.259736	-3063.342792	-3063.278643	-3063.432887	
W-L1^{Rh}-N-TS8	-3066.568234	-3065.615448	-3065.550492	-3065.706627	52.5
W-L1^{Rh}-N-TS10	-3066.582506	-3065.625735	-3065.560378	-3065.716477	46.3
W-L1^{Rh}-N-16	-3011.310373	-3010.368817	-3010.304432	-3010.459481	-17.3
Mo-L1^{Rh}-Cl-1'	-3766.888699	-3765.985102	-3765.922034	-3766.07328	
Mo-L1^{Rh}-Cl-TS8	-3769.243263	-3768.303706	-3768.239484	-3768.396484	21.5
Mo-L1^{Rh}-Cl-TS10	-3769.232485	-3768.289661	-3768.225122	-3768.380055	31.8
Mo-L1^{Rh}-Cl-16	-3713.942436	-3713.015371	-3712.951667	-3713.10597	-21.2
Mo-L1^{Rh}-N-1'	-3065.369032	-3064.452066	-3064.387886	-3064.542124	
Mo-L1^{Rh}-N-TS8	-3067.674078	-3066.721177	-3066.656272	-3066.812113	54.9
Mo-L1^{Rh}-N-TS10	-3067.68746	-3066.73105	-3066.665461	-3066.823105	48.0
Mo-L1^{Rh}-N-16	-3012.412026	-3011.470323	-3011.406751	-3011.560133	-12.0

Table S10 Computed energies (E), zero-point energy corrected energies (E_{zpe}), enthalpies (H) and Gibbs free energies (G; all in Hartree) of the selected intermediates and transition states at various DFT levels for the catalyst system **W-L1^{Rh}** as shown in Fig. S1.

Functional	Compd.	E	E_{zpe}	H	G	ΔG_{rel}
B97D3-BJ	H_2	-1.1829428	-1.173025	-1.16972	-1.17871	
	N_2	-109.4988745	-109.493463	-109.490158	-109.506089	
	NH_3	-56.5583513	-56.524939	-56.521127	-56.537173	
	1'	-2846.386837	-2845.471761	-2845.41274	-2845.555253	
	TS8	-2848.728621	-2847.778916	-2847.717604	-2847.866303	29.1
	TS10	-2848.7251	-2847.772405	-2847.710254	-2847.86233	31.6
	16	-2793.442194	-2792.502906	-2792.442712	-2792.587681	-21.0
PBE0-D3BJ	H_2	-1.1678393	-1.15782	-1.154515	-1.163506	
	N_2	-109.4414902	-109.435822	-109.432517	-109.448431	
	NH_3	-56.5199943	-56.48578	-56.481969	-56.498	
	1'	-2844.658062	-2843.720118	-2843.661867	-2843.803859	
	TS8	-2846.997635	-2846.023456	-2845.963818	-2846.108822	13.8
	TS10	-2846.979586	-2846.004216	-2845.943159	-2846.093963	23.2

		E	Ezpe	H	G	ΔGrel
	16	-2791.742675	-2790.780595	-2790.722518	-2790.863101	-41.9
B3LYP-D3BJ	H₂	-1.1793413	-1.169313	-1.166009	-1.174995	
	N₂	-109.5689086	-109.563311	-109.560007	-109.575924	
	NH₃	-56.5931105	-56.559181	-56.55537	-56.571403	
	1'	-2847.539988	-2846.604596	-2846.546559	-2846.68604	
	TS8	-2849.886395	-2848.916027	-2848.856141	-2849.001502	21.7
	TS10	-2849.875706	-2848.903492	-2848.842419	-2848.992275	27.5
	16	-2794.571007	-2793.612345	-2793.553159	-2793.696667	-35.8
M06-L	H₂	-1.1712078	-1.161368	-1.158063	-1.16705	
	N₂	-109.5531235	-109.547591	-109.544286	-109.56021	
	NH₃	-56.5753594	-56.541065	-56.537259	-56.55328	
	1'	-2847.001742	-2846.065588	-2846.007314	-2846.14751	
	TS8	-2849.319248	-2848.347967	-2848.287816	-2848.434594	29.5
	TS10	-2849.310896	-2848.335607	-2848.275191	-2848.422593	37.0
	16	-2794.016859	-2793.055826	-2792.997185	-2793.138331	-27.0

Table S11 Computed energies (E), zero-point energy corrected energies (E$_{zpe}$), enthalpies (H) and Gibbs free energies (G; all in Hartree) of the different stationary points involved in the direct hydrogenation of N$_2$ to NH$_3$ utilizing the catalysts **W-L4^{Rh}** and **W-L7^{Rh}** as shown in Fig. S3.

Compd.	E	E$_{zpe}$	H	G	ΔG$_{rel}$
H₂	-1.1829428	-1.173025	-1.16972	-1.17871	
N₂	-109.4988745	-109.493463	-109.490158	-109.506089	
NH₃	-56.5583513	-56.524939	-56.521127	-56.537173	
W-L4^{Rh}-1'	-4646.781917	-4645.864704	-4645.787789	-4645.981044	0.0
W-L4^{Rh}-2	-4647.949913	-4647.018583	-4646.940337	-4647.133588	16.4
W-L4^{Rh}-TS3	-4647.934427	-4647.005168	-4646.927505	-4647.120948	24.4
W-L4^{Rh}-4	-4647.954941	-4647.019704	-4646.941508	-4647.137275	14.1
W-L4^{Rh}-TS5	-4647.926759	-4646.994641	-4646.916847	-4647.112823	29.4
W-L4^{Rh}-6	-4647.957636	-4647.019626	-4646.941783	-4647.135998	14.9
W-L4^{Rh}-7	-4649.133127	-4648.180404	-4648.101133	-4648.298458	25.1
W-L4^{Rh}-TS8	-4649.121122	-4648.167621	-4648.089693	-4648.284719	33.7
W-L4^{Rh}-9	-4649.131648	-4648.173503	-4648.095773	-4648.290821	29.9
W-L4^{Rh}-TS10	-4649.110386	-4648.154906	-4648.076041	-4648.272839	41.2
W-L4^{Rh}-11	-4592.612327	-4591.694329	-4591.6196	-4591.807049	-3.6
W-L4^{Rh}-TS12	-4592.584646	-4591.662857	-4591.58689	-4591.776661	15.5
W-L4^{Rh}-13	-4592.635839	-4591.714058	-4591.637623	-4591.82646	-15.8
W-L4^{Rh}-14	-4593.803194	-4592.865146	-4592.787608	-4592.981282	-0.8

W-L4^{Rh}-TS15	-4593.796519	-4592.862728	-4592.785155	-4592.978593	0.9
W-L4^{Rh}-16	-4593.836675	-4592.893383	-4592.81627	-4593.006631	-16.7
W-L4^{Rh}-TS17	-4593.807907	-4592.8685	-4592.791581	-4592.98465	-2.9
W-L4^{Rh}-18	-4593.816565	-4592.870848	-4592.79378	-4592.986078	-3.8
W-L7^{Rh}-1'	-3770.333214	-3769.107969	-3769.02612	-3769.220511	0.0
W-L7^{Rh}-2	-3771.498424	-3770.256602	-3770.173773	-3770.369793	18.5
W-L7^{Rh}-TS3	-3771.492505	-3770.252977	-3770.170751	-3770.365768	21.0
W-L7^{Rh}-4	-3771.512552	-3770.267744	-3770.185071	-3770.382435	10.5
W-L7^{Rh}-TS5	-3771.498454	-3770.256737	-3770.174528	-3770.368643	19.2
W-L7^{Rh}-6	-3771.501169	-3770.254947	-3770.172179	-3770.368282	19.4
W-L7^{Rh}-7	-3772.668931	-3771.404985	-3771.321884	-3771.522402	34.8
W-L7^{Rh}-TS8	-3772.665223	-3771.405054	-3771.321868	-3771.519012	37.0
W-L7^{Rh}-9	-3772.676993	-3771.409924	-3771.326744	-3771.522886	34.5
W-L7^{Rh}-TS10	-3772.675798	-3771.410615	-3771.328036	-3771.522458	34.8
W-L7^{Rh}-11	-3716.178913	-3714.948921	-3714.867946	-3715.061194	-12.8
W-L7^{Rh}-TS12	-3716.159214	-3714.932403	-3714.852219	-3715.040816	0.0
W-L7^{Rh}-13	-3716.1627	-3714.932475	-3714.85181	-3715.042048	-0.8
W-L7^{Rh}-14	-3717.342014	-3716.096157	-3716.013672	-3716.208072	7.2
W-L7^{Rh}-TS15	-3717.33759	-3716.093068	-3716.011606	-3716.204221	9.6
W-L7^{Rh}-16	-3717.373635	-3716.122897	-3716.040492	-3716.235259	-9.9
W-L7^{Rh}-TS17	-3717.357124	-3716.104625	-3716.024679	-3716.212305	4.5
W-L7^{Rh}-18	-3717.36886	-3716.113669	-3716.031863	-3716.224646	-3.2

Table S12 Computed energies (E), zero-point energy corrected energies (E$_{zpe}$), enthalpies (H) and Gibbs free energies (G; all in Hartree) of various end-on (**Ln-1^E**) and side-on (**Ln-1^S**) N$_2$ coordinated molybdenum pincer complexes, as shown in Fig. S4.

Compd.	E	E$_{zpe}$	H	G	ΔG$_{rel}$
L1-1^E	-1868.079346	-1867.542363	-1867.507048	-1867.599249	
L1-1^S	-1868.050935	-1867.514098	-1867.478771	-1867.569936	18.4
L2-1^E	-2025.275301	-2024.627885	-2024.587533	-2024.687747	
L2-1^S	-2025.259168	-2024.612389	-2024.572057	-2024.671947	9.9
L10-1^E	-1946.694587	-1946.104061	-1946.065018	-1946.165633	
L10-1^S	-1946.665747	-1946.075799	-1946.036682	-1946.136283	18.4
L11-1^E	-2066.542206	-2066.022009	-2065.984735	-2066.081441	
L11-1^S	-2066.513411	-2065.994716	-2065.956925	-2066.05513	16.5

Table S13 Computed energies (E), zero-point energy corrected energies (E_{zpe}), enthalpies (H) and Gibbs free energies (G; all in Hartree) of the different stationary points involved in the direct hydrogenation of N_2 to NH_3 utilizing the catalyst **Mo-L1^{Rh}**, as shown in Fig. S5.

Compd.	E	E_{zpe}	H	G	ΔG_{rel}
H$_2$	-1.1829428	-1.173025	-1.16972	-1.17871	
N$_2$	-109.4988745	-109.493463	-109.490158	-109.506089	
NH$_3$	-56.5583513	-56.524939	-56.521127	-56.537173	
Mo-L1^{Rh}-1'	-2847.490266	-2846.574788	-2846.515182	-2846.659484	0.0
Mo-L1^{Rh}-2	-2848.664467	-2847.734136	-2847.673127	-2847.82087	10.9
Mo-L1^{Rh}-TS3	-2848.655929	-2847.728443	-2847.667852	-2847.815401	14.3
Mo-L1^{Rh}-4	-2848.673244	-2847.740827	-2847.679824	-2847.827435	6.8
Mo-L1^{Rh}-TS5	-2848.648083	-2847.71954	-2847.658305	-2847.808286	18.8
Mo-L1^{Rh}-6	-2848.665939	-2847.728288	-2847.667953	-2847.814231	15.0
Mo-L1^{Rh}-7	-2849.835487	-2848.884156	-2848.823021	-2848.970263	29.3
Mo-L1^{Rh}-TS8	-2849.826019	-2848.876877	-2848.815435	-2848.965217	32.4
Mo-L1^{Rh}-9	-2849.837721	-2848.883164	-2848.820961	-2848.972987	27.6
Mo-L1^{Rh}-TS10	-2849.824887	-2848.872202	-2848.810237	-2848.960775	35.2
Mo-L1^{Rh}-11	-2793.32335	-2792.405941	-2792.346001	-2792.492837	-8.2
Mo-L1^{Rh}-TS12	-2793.310872	-2792.398232	-2792.338645	-2792.483432	-2.3
Mo-L1^{Rh}-13	-2793.315812	-2792.399164	-2792.339398	-2792.485446	-3.6
Mo-L1^{Rh}-14	-2794.507258	-2793.573323	-2793.512481	-2793.6608	-1.5
Mo-L1^{Rh}-TS15	-2794.503792	-2793.572287	-2793.512021	-2793.658035	0.3
Mo-L1^{Rh}-16	-2794.539502	-2793.600664	-2793.540385	-2793.68578	-17.2
Mo-L1^{Rh}-TS17	-2794.523537	-2793.586588	-2793.526572	-2793.672271	-8.7
Mo-L1^{Rh}-18	-2794.530102	-2793.586995	-2793.527062	-2793.671583	-8.2

Table S14 Computed energies (E), zero-point energy corrected energies (E_{zpe}), enthalpies (H) and Gibbs free energies (G; all in Hartree) of the selected stationary points at different spin states, as shown in Fig. S6.

Metal	Compd.	E	E_{zpe}	H	G	ΔG_{rel}
W	**^{1}1**	-1866.972491	-1866.43535	-1866.39992	-1866.49321	0.0
	^{3}1	-1866.959284	-1866.42528	-1866.38894	-1866.48541	4.9
	^{5}1	-1866.924728	-1866.39447	-1866.35755	-1866.45556	23.6
	^{1}1'	-2846.386837	-2845.47176	-2845.41274	-2845.55525	0.0
	^{3}1'	-2846.373239	-2845.46235	-2845.40143	-2845.55016	3.2
	^{5}1'	-2846.343269	-2845.43343	-2845.37134	-2845.52838	16.9
	^{1}2	-2847.558247	-2846.62769	-2846.56673	-2846.71422	0.0
	^{3}2	-2847.545229	-2846.61697	-2846.55545	-2846.70527	5.6

		E	E$_{zpe}$	H	G	ΔG$_{rel}$
	^{5}**2**	-2847.532547	-2846.60788	-2846.5456	-2846.69857	9.8
Mo	^{1}**1**	-1868.079346	-1867.54236	-1867.50705	-1867.59925	0.0
	^{3}**1**	-1868.063446	-1867.52909	-1867.49298	-1867.58872	6.6
	^{5}**1**	-1868.025143	-1867.49559	-1867.45856	-1867.55636	26.9
	^{1}**1'**	-2847.490266	-2846.57479	-2846.51518	-2846.65948	0.0
	^{3}**1'**	-2847.473059	-2846.56246	-2846.50136	-2846.6517	4.9
	^{5}**1'**	-2847.4449	-2846.53476	-2846.47323	-2846.62536	21.4
	^{1}**2**	-2848.664467	-2847.73414	-2847.67313	-2847.82087	0.0
	^{3}**2**	-2848.649089	-2847.72078	-2847.65943	-2847.8082	8.0
	^{5}**2**	-2848.63357	-2847.70922	-2847.64619	-2847.80055	12.7

Table S15 Computed energies (E), zero-point energy corrected energies (E$_{zpe}$), enthalpies (H) and Gibbs free energies (G; all in Hartree) of selected stationary points with tungsten/molybdenum complexes containing the ligand **L1** in two different solvents, as shown in Table S1.

Functional	Compd.	E	E$_{zpe}$	H	G	ΔG$_{rel}$
CH$_3$CN	**H$_2$**	-1.1829428	-1.173025	-1.16972	-1.17871	
	N$_2$	-109.4988745	-109.493463	-109.490158	-109.506089	
	NH$_3$	-56.5583513	-56.524939	-56.521127	-56.537173	
	W-L1^{Rh}-1'	-2846.386837	-2845.471761	-2845.41274	-2845.555253	
	W-L1^{Rh}-TS8	-2848.728621	-2847.778916	-2847.717604	-2847.866303	29.1
	W-L1^{Rh}-TS10	-2848.7251	-2847.772405	-2847.710254	-2847.86233	31.6
	W-L1^{Rh}-16	-2793.442194	-2792.502906	-2792.442712	-2792.587681	-21.0
DMSO	**H$_2$**	-1.1824929	-1.172575	-1.16927	-1.178557	
	N$_2$	-109.4979483	-109.492537	-109.489232	-109.505459	
	NH$_3$	-56.5576715	-56.524258	-56.520447	-56.536789	
	W-L1^{Rh}-1'	-2846.374401	-2845.458768	-2845.399014	-2845.544197	
	W-L1^{Rh}-TS8	-2848.715726	-2847.765909	-2847.704616	-2847.853335	30.1
	W-L1^{Rh}-TS10	-2848.712079	-2847.759047	-2847.697014	-2847.848318	33.3
	W-L1^{Rh}-16	-2793.429998	-2792.490213	-2792.430179	-2792.57471	-19.8
CH$_3$CN	**Mo-L1^{Rh}-1'**	-2847.490266	-2846.574788	-2846.515182	-2846.659484	
	Mo-L1^{Rh}-TS8	-2849.826019	-2848.876877	-2848.815435	-2848.965217	32.4
	Mo-L1^{Rh}-TS10	-2849.824887	-2848.872202	-2848.810237	-2848.960775	35.2
	Mo-L1^{Rh}-16	-2794.539502	-2793.600664	-2793.540385	-2793.68578	-17.2
DMSO	**Mo-L1^{Rh}-1'**	-2847.477692	-2846.561795	-2846.502319	-2846.647927	
	Mo-L1^{Rh}-TS8	-2849.813123	-2848.86354	-2848.802299	-2848.951066	33.9
	Mo-L1^{Rh}-TS10	-2849.811946	-2848.859383	-2848.797362	-2848.948356	35.6
	Mo-L1^{Rh}-16	-2794.527277	-2793.587954	-2793.52773	-2793.673515	-16.8

Table S16 Computed energies (E), zero-point energy corrected energies (E_{zpe}), enthalpies (H) and Gibbs free energies (G; all in Hartree) of the stationary points involved in the dimerization reaction (**1→1^{di}**), as shown in Fig. S6.

Ligand	Compd.	E	E_{zpe}	H	G	ΔG_{rel}
W-L1	**1**	-1866.972491	-1866.43535	-1866.39992	-1866.49321	
	1^{di}	-3733.886041	-3732.81377	-3732.74138	-3732.91472	45.0
W-L10	**1**	-1945.5877	-1944.99699	-1944.95789	-1945.05938	
	1^{di}	-3891.116938	-3889.93799	-3889.85811	-3890.04787	44.5
W-L11	**1**	-2065.43536	-2064.91496	-2064.87759	-2064.97522	
	1^{di}	-4130.810109	-4129.77139	-4129.6951	-4129.87746	45.8
Mo-L1	**1**	-1868.079346	-1867.54236	-1867.50705	-1867.59925	
	1^{di}	-3736.084618	-3735.01221	-3734.94034	-3735.1104	55.3
Mo-L10	**1**	-1946.694587	-1946.10406	-1946.06502	-1946.16563	
	1^{di}	-3893.315723	-3892.1362	-3892.05702	-3892.24294	55.4
Mo-L11	**1**	-2066.542206	-2066.02201	-2065.98474	-2066.08144	
	1^{di}	-4133.008779	-4131.96972	-4131.89405	-4132.07255	56.7

Table S17 Computed energies (E), zero-point energy corrected energies (E_{zpe}), enthalpies (H) and Gibbs free energies (G; all in Hartree) of the stationary points involved in the dimerization reaction (**1→2^{di}**), as shown in Fig. S7.

Ligand	Compd.	E	E_{zpe}	H	G	ΔG_{rel}
	N$_2$	-109.4988745	-109.493463	-109.490158	-109.506089	
W-L1	**1**	-1866.972491	-1866.43535	-1866.39992	-1866.49321	
	2^{di}	-3624.467537	-3623.40409	-3623.33375	-3623.50211	-13.7
W-L10	**1**	-1945.5877	-1944.99699	-1944.95789	-1945.05938	
	2^{di}	-3781.698435	-3780.52821	-3780.45053	-3780.63472	-13.8
W-L11	**1**	-2065.43536	-2064.91496	-2064.87759	-2064.97522	
	2^{di}	-4021.392291	-4020.36233	-4020.28815	-4020.46494	-12.9
Mo-L1	**1**	-1868.079346	-1867.54236	-1867.50705	-1867.59925	
	2^{di}	-3626.668953	-3625.60436	-3625.53464	-3625.70205	-6.1
Mo-L10	**1**	-1946.694587	-1946.10406	-1946.06502	-1946.16563	
	2^{di}	-3783.8997	-3782.72835	-3782.65117	-3782.83351	-5.2
Mo-L11	**1**	-2066.542206	-2066.02201	-2065.98474	-2066.08144	
	2^{di}	-4023.593836	-4022.56427	-4022.491	-4022.66427	-4.7

Table S18 Computed energies (E), zero-point energy corrected energies (E_{zpe}), enthalpies (H) and Gibbs free energies (G; all in Hartree) of the selected stationary points, as shown in Fig. S8.

Ligand	Compd.	E	E_{zpe}	H	G	ΔG_{rel}
	H_2	-1.1829428	-1.173025	-1.16972	-1.17871	
W-L1	1'	-2846.386837	-2845.471761	-2845.41274	-2845.55525	0.0
	2	-2847.558247	-2846.627689	-2846.566725	-2846.71422	12.4
	TS3	-2847.552404	-2846.62469	-2846.564181	-2846.71168	14.0
	4	-2847.574311	-2846.641092	-2846.579944	-2846.72904	3.1
	1^{H_2}	-2847.574874	-2846.645305	-2846.584567	-2846.731536	1.5
	2^{H_2}	-2848.762995	-2847.817474	-2847.755599	-2847.904948	4.8
	$TS3^{H_2}$	-2848.739477	-2847.79783	-2847.73631	-2847.885947	16.8
	4^{H_2}	-2848.743103	-2847.797163	-2847.73499	-2847.887203	16.0
Mo-L1	1'	-2847.490266	-2846.574788	-2846.515182	-2846.65948	0.0
	2	-2848.664467	-2847.734136	-2847.673127	-2847.82087	10.9
	TS3	-2848.655929	-2847.728443	-2847.667852	-2847.8154	14.3
	4	-2848.673244	-2847.740827	-2847.679824	-2847.82744	6.8
	1^{H_2}	-2848.66988	-2847.74033	-2847.679808	-2847.826104	7.6
	2^{H_2}	-2849.859854	-2848.915094	-2848.853146	-2849.00236	9.1
	$TS3^{H_2}$	-2849.832196	-2848.890766	-2848.829209	-2848.979554	23.0
	4^{H_2}	-2849.833913	-2848.888016	-2848.826299	-2848.975316	26.1

10 Literature

1   M. J. Frisch, G. W. Trucks, H. B. Schlegel, G. E. Scuseria, M. A. Robb, J. R. Cheeseman, G. Scalmani, V. Barone, G. A. Petersson, H. Nakatsuji, X. Li, M. Caricato, A. V. Marenich, J. Bloino, B. G. Janesko, R. Gomperts, B. Mennucci, H. P. Hratchian, J. V. Ortiz, A. F. Izmaylov, J. L. Sonnenberg, D. Williams-Young, F. Ding, F. Lipparini, F. Egidi, J. Goings, B. Peng, A. Petrone, T. Henderson, D. Ranasinghe, V. G. Zakrzewski, J. Gao, N. Rega, G. Zheng, W. Liang, M. Hada, M. Ehara, K. Toyota, R. Fukuda, J. Hasegawa, M. Ishida, T. Nakajima, Y. Honda, O. Kitao, H. Nakai, T. Vreven, K. Throssell, J. A. Montgomery, Jr., J. E. Peralta, F. Ogliaro, M. J. Bearpark, J. J. Heyd, E. N. Brothers, K. N. Kudin, V. N. Staroverov, T. A. Keith, R. Kobayashi, J. Normand, K.

Raghavachari, A. P. Rendell, J. C. Burant, S. S. Iyengar, J. Tomasi, M. Cossi, J. M. Millam, M. Klene, C. Adamo, R. Cammi, J. W. Ochterski, R. L. Martin, K. Morokuma, O. Farkas, J. B. Foresman, and D. J. Fox, Gaussian 16, Revision B.01., Wallingford CT, 2016.

2   A. V Marenich, C. J. Cramer and D. G. Truhlar, *J. Phys. Chem. B*, 2009, **113**, 6378–6396.

3   A. D. Becke, *J. Chem. Phys.*, 1997, **107**, 8554–8560.

4   S. Grimme, *J. Comput. Chem.*, 2006, **27**, 1787–1799.

5   S. Grimme, J. Antony, S. Ehrlich and H. Krieg, *J. Chem. Phys.*, 2010, **132**, 154104.

6   S. Grimme, S. Ehrlich and L. Goerigk, *J. Comput. Chem.*, 2011, **32**, 1456–1465.

7   A. Schäfer, C. Huber and R. Ahlrichs, *J. Chem. Phys.*, 1994, **100**, 5829–5835.

8   A. Schäfer, H. Horn and R. Ahlrichs, *J. Chem. Phys.*, 1992, **97**, 2571–2577.

9   F. Weigend and R. Ahlrichs, *Phys. Chem. Chem. Phys.*, 2005, **7**, 3297–3305.

10   D. Andrae, U. Haeussermann, M. Dolg, H. Stoll and H. Preuss, *Theor. Chim. Acta*, 1990, **77**, 123–141.

11   A. D. Becke, *J. Chem. Phys.*, 1992, **96**, 2155–2160.

12   J. P. Perdew, K. Burke and M. Ernzerhof, *Phys. Rev. Lett.*, 1996, **77**, 3865.

13   P. J. Stephens, F. J. Devlin, C. F. Chabalowski and M. J. Frisch, *J. Phys. Chem.*, 1994, **98**, 11623–11627.

14   C. Lee, W. Yang and R. G. Parr, *Phys. Rev. B*, 1988, **37**, 785.

15   Y. Zhao and D. G. Truhlar, *J. Chem. Phys.,* 2006*,* **125**, 194101–194117*.*